Journal of Luminescence 133 (2013) 268–275

Contents lists available at SciVerse ScienceDirect

Journal of Luminescence

journal homepage: www.elsevier.com/locate/jlumin

Frontiers of mid-infrared lasers based on transition metal doped II–VI semiconductors

S. Mirov [a,b,*], V. Fedorov [a], I. Moskalev [b], M. Mirov [b], D. Martyshkin [a]

[a] Department of Physics, University of Alabama at Birmingham, Birmingham, AL 35294, USA
[b] IPG Photonics, Mid-Infrared Lasers, 1500 1st Ave N., Unit 39, Birmingham, AL 35203, USA

ARTICLE INFO

Available online 22 September 2011

Keywords:
Tunable lasers
Mid-IR lasers
Transitional metal doped lasers
II–VI semiconductors
Cr:II–VI crystals
Fe:II–VI crystals

ABSTRACT

Recent progress in chromium and iron doped II–VI semiconductor materials makes them the laser sources of choice when one needs a compact system with broad mid-IR tunability over 1.9–6 μm. Output powers exceeding 10 W, output energies 20 mJ, pulse durations 80 fs, peak powers in excess of 1 GW, and efficiency up to 70% were demonstrated in several Cr doped semiconductors. The unique combination of technological and spectroscopic characteristics makes these materials ideal candidates for mid-IR tunable and ultrafast laser systems. This article reviews transition metal doped II–VI materials and recent progress in Cr- and Fe- doped solid-state mid-IR lasers.

1. Introduction

Middle-infrared (mid-IR) wavelengths are usually generated using relatively complex nonlinear optical conversion techniques or by means of direct generation in hetero-junction lead-salt, antimonide, or quantum cascade semiconductor lasers featuring limited output power and tuning range. Impurity doped crystalline lasers constitute another viable route for mid-IR coherent sources. Transition metal (TM^{2+}, e.g., Cr^{2+} or Fe^{2+}) doped binary (e.g., ZnSe, ZnS, CdSe, CdS, ZnTe) and ternary (e.g., CdMnTe, CdZnTe, ZnSSe) chalcogenide crystals, having a gain bandwidth up to 50% of central wavelength, represent another class of solid state gain media with strong and ultra-broad absorption and emission bands in the mid-IR range of optical spectra.

2. Spectroscopic properties of ^{5}D ions in II–VI semiconductors

2.1. Physical properties of II–VI semiconductors

Wide-bandgap II–VI semiconductors are well known materials for infrared windows, fabrication of light-emitting devices (LED), phosphors for electro-luminescent displays, and photovoltaic devices for a variety of photonics applications. Another important application area of TM doped II–VI devices is a spintronics. The diluted magnetic semiconductors (DMSs) have been intensively investigated for many years. Most of the early papers were devoted to materials doped by Mn, Fe, and Co ions. DMS structures in $Zn_{1-x}Mn_xSe$ and $Zn_{1-x}Fe_xSe$/ZnSe superlattices were studied in Refs. [1–3].

For most of the above applications, the chromium and iron ions were considered as undesirable impurities. Therefore the doping procedure with concentration and optical quality suitable for laser applications had not been developed until the first laser experiments demonstrated in the middle of 90's. Currently, the most frequently used fabrication methods for Iron and Chromium doped II–VI materials are: post growth thermal diffusion, physical vapor transport, Bridgman method, and hot-pressed ceramic.

Two features of TM doped II–VI materials are especially important for mid-IR laser applications [4]. First of all, tetrahedral symmetry of the TM ions gives approximately twice smaller crystal field splitting, placing the TM dopant transitions further into the IR. Secondly, low energy optical phonon cut-off makes them transparent in a wide spectral region and decreases non-radiative relaxation. The material properties of the most important II–VI crystals are summarized in Table 1.

2.2. Spectroscopic properties of ^{5}D ions

The ground state of free Cr^{2+} ($3d^4$) and Fe^{2+}($3d^6$) ions is ^{5}D state with spin (S) and orbital (L) numbers equal to 2; and degeneracy $g=(1+2L)(1+2S)=25$. Energy gaps to the other terms of free ions (^{3}H, ^{3}G, ^{3}F(2), ^{3}D, ^{3}P(2), ^{1}I, ^{1}G(2), ^{1}F, ^{1}D(2), ^{1}S(2)) can be calculated using only two Racah parameters: B and C. Empirical values of the Racah parameters for Cr^{2+}(Fe^{2+}) are equal to $B=830(1058)$ and $C=3430(3901)$ cm^{-1}, correspondingly [5]. The tetrahedral crystal field (T_d) of the II–VI semiconductors splits ^{5}D ground state into triplet $^5T_2$ and duplet ^{5}E. In the weak

* Corresponding author at: University of Alabama at Birmingham, Department of Physics, Birmingham, AL 35294, USA. Tel.: +1 205 934 8088; fax: +1 205 934 8042.
E-mail address: mirov@uab.edu (S. Mirov).

0022-2313/$ - see front matter © 2011 Elsevier B.V. All rights reserved.
doi:10.1016/j.jlumin.2011.09.040

Table 1
Materials properties of ZnS, ZnSe, CdSe, and CdMnTe crystals (C-Cubic symmetry; H-Hexagonal symmetry).

Crystal	ZnS	ZnSe	CdSe	CdMnTe
Symmetry	C/H	C	H	C
Density, g/cm^3	4.08	5.26	5.81	
Bond length, nm	0.234	0.245	0.263	0.276
Band gap, eV	3.9	2.8	1.7	2.1
Max phonon ν_{LO}, cm^{-1}	330	250	218	~200
Transparency range, μm	0.4–14	0.5–20	0.8–21	0.6–22
n @3.0 μm	2.26	2.44	2.5	2.5
$(1/n)(dn/dT)$, K^{-1}	1.9×10^{-5}	2.6×10^{-5}	4×10^{-5}	
Second order nonlinearity, pV/m	d_{eff}=8	d_{eff}=30	d_{31}=35	d_{14}=340
Third order of nonlinearity, 10^{-20} m^2/W	84	460	1300	
	@1.06 μm	@1.06 μm	@1.5 μm	
Verdet constant, Deg/Tm	3024	6700	3300	20000
	@0.63 μm	@0.63 μm	@0.98 μm	@0.98 μm
Specific heat, J/gK	0.47	0.34	0.49	
Thermal conductivity, W/cm K	0.27	0.19	0.09	0.075
Hardness, Knoop	178	100	44–90	62 (Vickers)

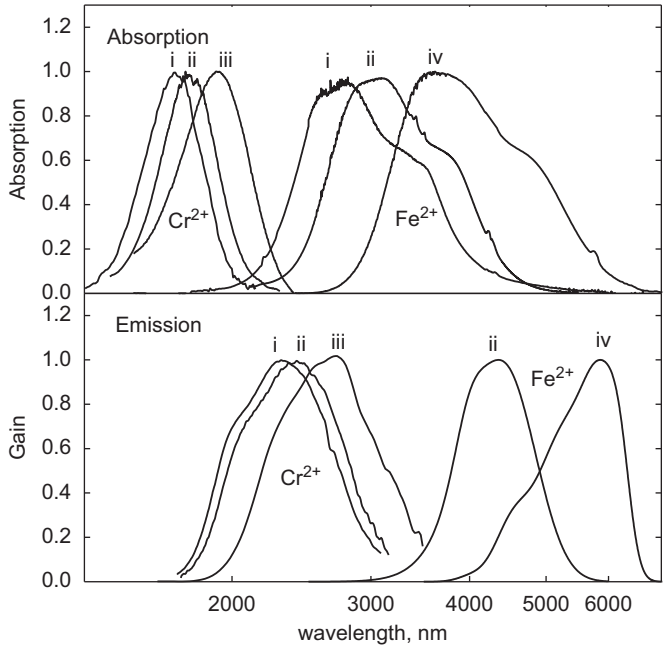

Fig. 1. Normalized room temperature absorption and emission-gain spectra of Cr^{2+} and Fe^{2+} ions in ZnS (i), ZnSe (i), CdSe(iii); and CdMnTe (iv) crystals.

strength crystal field (with crystal field parameter $Dq<1.2$ B), these two levels are the lowest. The doublet ^{5}E is the ground state of the Fe^{2+} ions, while $^5T_2$ is the ground state of the Cr^{2+} ions. Energy splitting between these levels using crystal field theory is described as [5].

$$\Delta = E(^5E) - E(^5T_2) = 10Dq = \left(\frac{20}{27}\right)\frac{Q^2}{4\pi\varepsilon_0 a^5}\langle r^4\rangle_{3d} \quad (1)$$

where Q is a ligand's charge; a is the distance between ligands and transition metals; r is the radius of the 3d-electrons. All other terms have spin smaller than 2; therefore, transitions from the components of the ^{5}D term to other terms are spin forbidden. Transitions between ^{5}D components are spin-allowed. Absorption and emission spectra at $^5E\leftrightarrow{}^5T_2$ transition of some chromium-doped II–VI crystals are depicted in Fig. 1. Major spectroscopic characteristics of chromium and iron ions in ZnS, ZnSe, CdSe, and CdMnTe crystals are summarized in Table 2.

Among II–VI chalcogenides ZnS crystals feature maximum ^{5}D term energy splitting due to the smallest inter-ligand distance

Table 2
Spectroscopic characteristics of chromium and iron ions in ZnS, ZnSe, CdSe, and CdMnTe crystals [4,6–10]. σ_{ab}, σ_{em},—peak absorption and emission cross-sections; λ_{ab}, λ_{em}—peak absorption and emission cross-section wavelengths, respectively; τ_{rad}—radiative lifetime.

	Cr^{2+}			Fe^{2+}	
	ZnS	ZnSe	CdSe	ZnSe	$Cd_{1-x}Mn_xTe$
Dq, cm^{-1}	465	443		*293*	248(x=0)
Absorption					
σ_{ab}, 10^{-20} cm^2	100	110	194	97	52
λ_{ab}, nm	1690	1770	1890	3100	3600
$\Delta\lambda_{ab}$, nm	350	350	440	1330	1910
Emission					
σ_{em}, 10^{-20} cm^2	140	130	200	153	140
λ_{em}, nm	2350	2450	2650	4350	5760
$\Delta\lambda_{em}$, nm	820	860	940	1610	1400
τ_{rad}, μs	5.7	5.5	6.4	57	75
τ_{RT}, μs	4.3	5.4	4.4	0.37	0.17
$\eta=\tau_{RT}/\tau_{rad}$	0.8	~1	0.7	1.5×10^{-3}	2×10^{-3}

(see Fig. 1 and Table 2). Therefore, the absorption and emission bands of Cr $^5E\leftrightarrow{}^5T_2$ transition in ZnS are shifted to shorter wavelengths in comparison with the bands of other II–VI semiconductors. On the other hand, crystals with Cd and Te elements featuring one of the biggest lattice parameter have the longest absorption and emission band among this group. The radiative lifetimes of chromium doped ZnSe, ZnS, CdSe crystals can be estimated as a low-temperature limit of kinetics of luminescence depicted in Fig. 2. There is no luminescence quenching in ZnSe crystal at RT, which means that the luminescence quantum yield is close to unity in this crystal. RT fluorescence lifetime of Cr^{2+} in ZnS and CdSe crystals drops by ~20–30% in comparison with low temperature measurements. The radiation lifetimes at $^5E\rightarrow{}^5T_2$ transition of chromium ions in ZnSe, ZnS, and CdSe hosts are very close and equal to ~6 μs. Emission cross-sections could be estimated from the luminescence spectra and radiative lifetime measurements with the use of Füchtbauer-Ladenburg equation. The maximum values of chromium emission cross-sections are larger than 10^{-18} cm^2 for all II–VI hosts.

Iron ions reveal thermal quenching of the mid-IR luminescence at RT in all studied semiconductors due to a small crystal field splitting. The longest kinetics of the luminescence was measured in the Fe:ZnSe crystal and was equal to 370 ns. Temperature dependence of luminescence lifetime for the low doped sample ($C_{Fe}=0.1\times10^{18}$ cm^{-3}) shows that the radiative